Journal of Environmental Chemical Engineering 12 (2024) 112995

Contents lists available at ScienceDirect

Journal of Environmental Chemical Engineering

journal homepage: www.elsevier.com/locate/jece

Bubble-less photocatalytic ozonation with ceramic membranes and static mixers enhances the total organic carbon removal and degradation of iodinated X-ray contrast agents

Stefan Herrmann [a], Konstantin Dietz [a], Lennart Wilms [a], Matthias Wessling [a,b,*]

[a] RWTH Aachen University, Forckenbeckstraße 51, Aachen 52074, Germany
[b] DWI - Leibniz Institute for Interactive Materials, Forckenbeckstraße 50, Aachen 52074, Germany

ARTICLE INFO

Keywords:
Membrane Contactor
Micropollutants
Photocatalytic Ozonation
Static Mixers
TOC Removal

ABSTRACT

Conventional bubble-based ozonation of wastewater creates several issues, e.g., the low degradation of certain micropollutants like X-ray contrast agents, mass transfer limitations due to inhomogeneous mixing, and the waste of undissolved ozone. In contrast, this work uses tubular ceramic membranes for bubble-free and bubble-less ozonation. Static mixers are placed around the membrane to enhance the radial mixing of ozone, creating homogeneous reaction conditions throughout the membrane contactor. Additionally, the ozone mass transfer significantly increases with static mixers. Furthermore, the membrane is made of a photocatalyst (TiO_2) on the shell-side to improve the micropollutant degradation by photocatalytic ozonation. An ozone-stable hydrophobic treatment method is developed to use ceramic membranes as a membrane contactor for the ozonation of water. After hydrophobic treatment, the ozone mass transfer coefficient is in the order of $1.3 \cdot 10^{-6}$ ms^{-1} using bubble-less operation resulting in an ozone concentration up to 4.0 mg L^{-1}. Overall, bubble-less operation significantly increases the ozone mass transfer compared to bubble-free operation. Photocatalytic ozonation in a membrane contactor with static mixers increases the degradation of diatrizoate by 37% compared to sole ozonation in the same membrane contactor. Furthermore, this process increases the removal of total organic carbon in experiments with a water matrix consisting of four different micropollutants by 115% compared to sole ozonation.

1. Introduction

Micropollutants (MPs) are a severe hazard to the aquatic environment, whole ecosystems, and potable water supply [1]. However, MPs are found in many water bodies around the world, and the documented MP levels are rising with industrial progress and increasing prosperity of the global population [2,3]. MPs are anthropogenic organic substances that are persistent, bioaccumulative, and harmful to living organisms [4,5]. Due to their chemical stability, conventional wastewater treatment plants (WWTP) are not able to remove or degrade MPs [6]. Thus, technologies need to be identified that are capable of efficiently degrading MPs without producing other potentially harmful by-products [7].

One group of MPs are pharmaceuticals and their metabolic products. Due to an aging society and increasing prosperity, the consumption of pharmaceuticals is significantly growing [8,9]. Thus, substances like antibiotics, e.g., sulfamethoxazole (SMX), anticonvulsants, e.g., carbamazepine (CBZ), anti-inflammatory drugs, e.g., diclofenac (DCF), and iodinated X-ray contrast agents, e.g., diatrizoate (DTA) are detectable in the range of 0.1 μg L^{-1} to 1 μg L^{-1} in WWTP effluents [10–12]. Ending up in surface water and drinking water, these substances pose a severe health hazard for microorganisms, animals, and humans. Furthermore, the low concentration impedes their efficient degradation. Hence, it is an option to tackle the problem at main point sources for pharmaceutical MPs, i.e., hospitals. Hospital effluents show concentrations of pharmaceutical MPs in the order of 0.2 μg L^{-1} to 1000 μg L^{-1} [13]. Especially iodinated X-ray contrast agents are detected at high levels of 100 μg L^{-1} to 3000 μg L^{-1}. These iodinated X-ray contrast agents are known to be very stable and challenging to degrade even with advanced oxidation processes (AOP) [14]. DTA, as an ionic X-ray contrast agent, is known to be the most stable of its kind [15]. Thus, technologies that can degrade highly stable pharmaceuticals are desperately needed to protect water bodies.

As a countermeasure to increasing MP levels, AOPs become necessary as an additional treatment stage in WWTPs. Ozonation is a possible

* Corresponding author at: RWTH Aachen University, Forckenbeckstraße 51, Aachen 52074, Germany.
E-mail address: Manuscripts.CVT@avt.rwth-aachen.de (M. Wessling).

https://doi.org/10.1016/j.jece.2024.112995
Received 10 January 2024; Received in revised form 3 April 2024; Accepted 5 May 2024
Available online 8 May 2024

Nomenclature

Abbreviations

AOP	Advanced oxidation process
CBZ	Carbamazepine
DAD	Diode-array detector
DCF	Diclofenac
DI	Deionized
DTA	Diatrizoate
EDX	Energy-dispersive X-ray spectroscopy
FESEM	Field emission scanning electron microscop
HPLC	High-performance liquid chromatography
LED	Light-emitting diode
MP	Micropollutant
PFAS	Per- and polyfluoroalkyl substances
PTFE	Polytetrafluoroethylene
SMX	Sulfamethoxazole
TOC	Total organic carbon
UV	Ultraviolet
WWTP	Wastewater treatment plant

Symbols

A_{mem}	Surface area of the membrane
c_g	Concentration in gas phase
$c_{l,out}$	Concentration in liquid phase at reactor outlet
e^-	Excited electron
h^+	Electron hole
H_S^{cc}	Henry coefficient
K_L	Mass transfer coefficient
Re	Reynolds number
$\dot{V}$	Volume flow rate
$wt-\%$	Weight percent

technology that is thoroughly investigated from lab-scale to pilot-scale and has already been implemented in several full-scale WWTPs [16,17]. While ozone selectively reacts with specific molecule structures comprising nucleophilic moieties (i.e., aromatic rings, carbon-carbon double bonds, and some functional groups) [18], hydroxyl radicals ($OH^\bullet$) and other oxidizing species that occur during ozone decay (e.g., $O_2^{\bullet-}$, $O_3^{\bullet-}$), react non-selectively with MPs and can result in complete mineralization of the MPs [18,19].

Due to the lower oxidation potential of ozone and its reactive selectivity, the reaction to hydroxyl radicals and other oxidizing species is promoted in ozone-based AOPs. Therefore, either additional reactants, i.e., hydrogen peroxide, are dosed into the ozonation reactor [20,21], or ozone decay is accelerated by catalytic ozonation [22,23], or photocatalytic ozonation [24–26].

In photocatalytic ozonation, as illustrated in Figure 1, a photocatalyst, e.g., TiO_2, is used. Excited electrons (e^-) of the photocatalyst can react with ozone to $O_3^{\bullet-}$, which can directly react with MPs or with water to hydroxyl radicals [24]. Furthermore, excited electrons can directly react with MPs or with dissolved oxygen to $O_2^{\bullet-}$ radicals that subsequently react with MPs. Electron holes (h^+) directly react in water with MPs or generate hydroxyl radicals that can subsequently react with MPs [27]. Overall, photocatalytic ozonation accelerates ozone decay to other oxidizing species and creates additional oxidizing species at the photocatalyst [24]. Thus, a more comprehensive range of MPs can be degraded using photocatalytic ozonation compared to sole ozonation [24].

Furthermore, the formation of harmful by-products, i.e., bromate, can be reduced using photocatalytic ozonation, compared to ozonation [28]. Bromate formation can be significantly lowered by decreasing the local ozone concentration. This can be achieved by promoting ozone decay reactions to other reactive species, e.g., hydroxyl radicals, by photocatalytic ozonation without affecting the degradation of MPs [28,29]. Another strategy to lower the local dissolved ozone concentration is preventing ozone hotspots and intensifying mixing in the ozonation reactor by reactor design [30].

Conventional wastewater ozonation is conducted in bubble columns, or with venturi injectors [31,32]. However, these reactor types are unsuitable for efficient photocatalytic ozonation due to the unfavourable surface-to-volume ratio for UV light input. Furthermore, the photocatalyst needs to be added as suspended particles that further limit the penetration depth of UV light and the particles must be separated from the wastewater stream after the reactor in an additional, energy-demanding filtration step [27,33]. Hence, an immobilized photocatalyst is a viable alternative. Ceramic membranes, made of a photocatalytic material, e.g., TiO_2, can be used for this purpose [34,35]. Furthermore, these membranes are ozone-stable and can be simultaneously used as a membrane contactor for bubble-less ozonation, as shown in principal in Figure 1. Thus, problems arising from bubble-based ozonation, i.e., bromate formation and undissolved ozone in an off-gas stream, can be tackled with this technology [36,37].

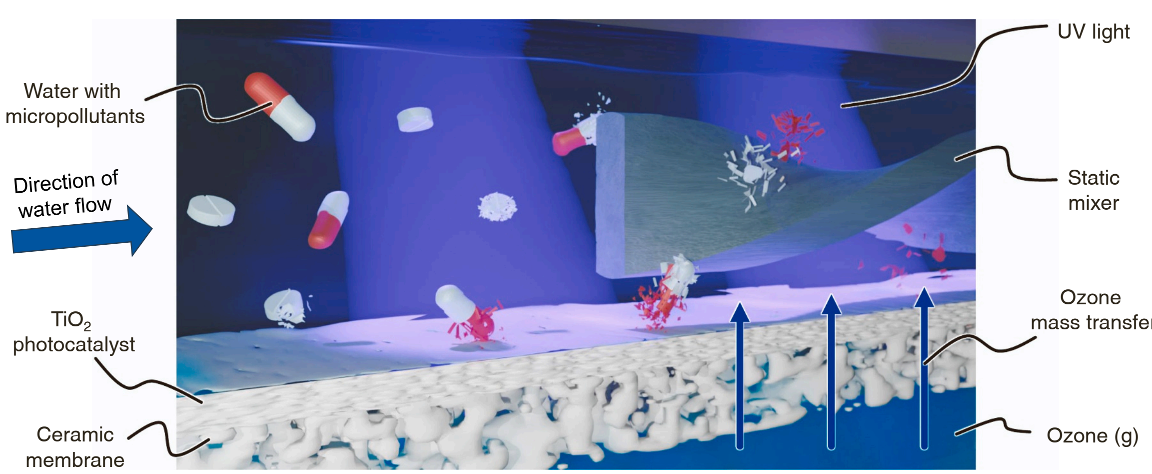

Fig. 1. Principal of membrane-based photocatalytic ozonation. The hydroxyl radical concentration increases at the membrane's surface due to photocatalytic reactions with water and photocatalytic ozone decay. Thus, micropollutant degradation is promoted. Furthermore, ozone mass transfer is bubble-less and mainly based on diffusion at the phase boundary of ozone gas and water at the membrane's surface.

However, the use of hydrophilic ceramic membranes as a membrane contactor requires a hydrophobic treatment to prevent flooding of the membrane and, consequently, a significant decrease in ozone mass transfer [38,39]. Different hydrophobic treatment methods are reported in the literature, most of which focus on fluorinated silanes [40,41] or coating layers of a hydrophobic material, e.g., polytetrafluoroethylene (PTFE) [42]. These coatings make ceramic membranes suitable for membrane-based photocatalytic ozonation.

To date, photocatalytic ozonation is limited to lab-scale studies. Batch reactors with suspended TiO_2 as photocatalyst are primarily used, and ozone is added to the reactor by bubbling ozone gas into the suspension [28,43–46]. In contrast, Rodriguez et al. [47] and Moreira et al. [48] used immobilized TiO_2 on a support structure to eliminate a subsequent separation process of the suspended TiO_2 particles. Thus, the complexity and the operational costs in terms of energy consumption of the overall process are reduced. However, they used separate reactors for bubble-based ozone supply and photocatalysis, and water was subsequently pumped through both reactors. To optimize photocatalytic ozonation, it would be best to combine ozonation and photocatalysis using an immobilized photocatalyst within one reactor. However, little literature is found using such reactors. Presumido et al. [25] present a membrane contactor for photocatalytic ozonation. They coated TiO_2 onto a membrane to create a reactor combining immobilized photocatalyst and ozonation. However, ozone mass transfer is still based on micro-sized bubbles created by the porous membrane. He et al. [49] built a microfluidic membrane reactor for photocatalytic ozonation using a porous TiO_2 layer on carbon paper. This membrane contactor is operated bubble-free, and ozone is dissolved by diffusion through the membrane. Thus, the interference of bubbles in water with UV light is eliminated, increasing the photocatalytic efficiency of the process. Furthermore, they show that a gas-side PTFE coating creates sufficient hydrophobicity to prevent flooding of the membrane. Overall, publications show a significant increase in the degradation of a wide range of micropollutants using photocatalytic ozonation [24].

This work presents a tubular membrane contactor for bubble-less photocatalytic ozonation using a ceramic Al_2O_3 membrane with a selective layer made of TiO_2. Furthermore, a coating method to obtain hydrophobic properties of a ceramic is adapted and optimized for use in ozonation. The ozone mass transfer behavior and the degradation of DTA and three other MPs are studied using the membrane contactor with static mixers and photocatalytic ozonation. Three hypotheses are to be proved in this work. First, coating the support layer of a ceramic membrane with PTFE particles creates sufficient hydrophobicity for use as an ozone membrane contactor. Second, ceramic TiO_2 membranes are suitable as a membrane contactor and immobilized catalyst in bubble-less photocatalytic ozonation. Third, implementing static mixersand using photocatalytic ozonation enhances ozone mass transfer, micropollutant degradation, and total organic carbon (TOC) removal compared to sole ozonation.

2. Material and Methods

2.1. Hydrophobic treatment of ceramic membranes

Ceramic membranes with a support layer of Al_2O_3, a shell-side selective layer of pure TiO_2, and a pore size of 50 nm (atech innovations GmbH, Germany) are used for all experiments in this work. The membranes have an outer diameter of 10 mm, an inner diameter of 6 mm and a length of 500 mm. Both ends of the membranes are PTFE sealed to allow gas-tight assembly of the membrane in the reactor. The crystal structure of TiO_2 on the shell-side of the membrane is 80% anatase and 20% rutile, according to the manufacturer.

Adding a hydrophobic treatment to the intrinsically hydrophilic ceramic membranes is necessary to use them as a membrane contactor in ozonation. Therefore, a method presented by Xu et al. [42] is modified and used in this work. An aqueous PTFE dispersion (Sigma-Aldrich / Merck, Germany) with 60 wt.-% PTFE particles is diluted with isopropanol to a concentration of 0.1 wt.-%. 200 mL of the diluted PTFE dispersion are filtrated through the membrane, either outside-in (on the selective layer) or inside-out (into the support layer) by vacuum filtration. Figure 2 shows the coating setup for support layer coating. The membrane is placed in a vacuum-tight vessel, connected to a reservoir with the PTFE dispersion and vacuum is applied to the shell-side of the membrane. PTFE particles accumulate at the boundary of the support and selective layer, as the particles are larger than the pores of the selective layer. Thus, a hydrophobic barrier is applied into the membrane. For selective layer coating, the membrane is submerged in the PTFE dispersion and vacuum is applied to the lumen channel. The PTFE particles accumulate on the selective layer and form a hydrophobic layer on the shell-side of the membrane. Membranes that are coated on the selective layer are sintered at 335 ˚C for 10 min under argon atmosphere to form a cohesive layer on the shell-side. Membranes with support layer coating are dried for at least 24 h at room temperature prior to use.

2.2. Tubular membrane contactor

For photocatalytic ozonation, the contactor housing enclosing the ceramic membrane must be ozone-stable and have a high UV transmission to apply UV radiation from the outside. Figure 3 shows the assembly of the membrane contactor. A fused silica tube (QCS GmbH, Germany) with a length of 400 mm, an outer diameter of 28 mm, an inner diameter of 22 mm, and KF25 connections (DIN 28403) on both sides is used as main part of the housing. A potting element is connected on each side to the fused silica tube with the KF25 connection and a related centering ring and clamp.

The potting elements are tailor-made for this application; the technical drawings are presented in the SI. Aluminum is used to fabricate the potting elements and the respective lids using a lathe. The potting elements separate the gas-side and the liquid side of the membrane contactor, seal the membrane gas-tight into the contactor setup, and provide tube connections for the ozone supply and the water circuit. For sealing the membrane, an FKM O-ring 9.5 mm × 2.5 mm is used. The O-ring is placed onto the membrane and compressed by the potting lid to ensure gas-tight sealing. The lid of the potting element is sealed with an additional O-ring. Pristine O-rings are used for every single experiment. The active membrane length for mass transfer in the membrane contactor between both potting elements is 460 mm.

To increase radial mixing in the membrane contactor, static mixers are used. The static mixers are placed in the void volume between the membrane and the fused silica housing. They are Kenics type with an element length of 20 mm and a diameter of 4.5 mm. Six circular-arranged static mixers form one static mixer element with a length of 100 mm. The six static mixers are connected with a ring structure on each end of the static mixer element. Four of these elements are placed in a row into the membrane contactor for experiments with static mixers. The static mixers are 3D printed from either polymeric High Temp resin (Formlabs, United States) or aluminum (Xometry Europe GmbH, Germany).

2.3. Water treatment experiments

The membrane contactor is used in an open-loop configuration, according to Figure 4 a), to characterize the ozonation behavior of the ceramic membrane with a hydrophobic coating. Pure oxygen (Westfalen AG, Germany) is fed to an adjustable ozone generator BMT 802 N (BMT Messtechnik GmbH, Germany) to generate an ozone oxygen mixture. The ozone content of the mixture is measured by an ozone analyzer BMT 964 (BMT Messtechnik GmbH, Germany) before it enters the lumen-side of the membrane contactor. This measurement is used to adjust the power settings of the ozone generator, ensuring the desired, constant gaseous ozone concentration during each experiment. A back pressure regulator KBP1 (Swagelok, United States) on the gas-side behind the

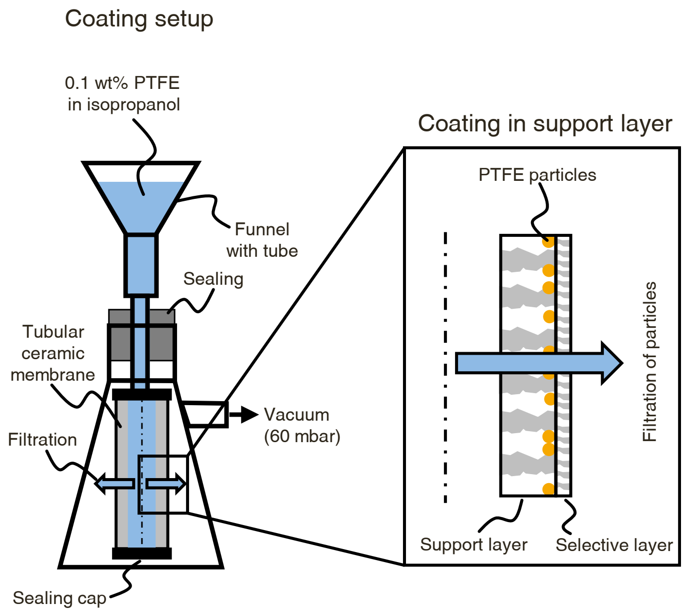

Fig. 2. Setup for hydrophobic coating of ceramic membranes with vacuum filtration using PTFE particles in an isopropanol solution.

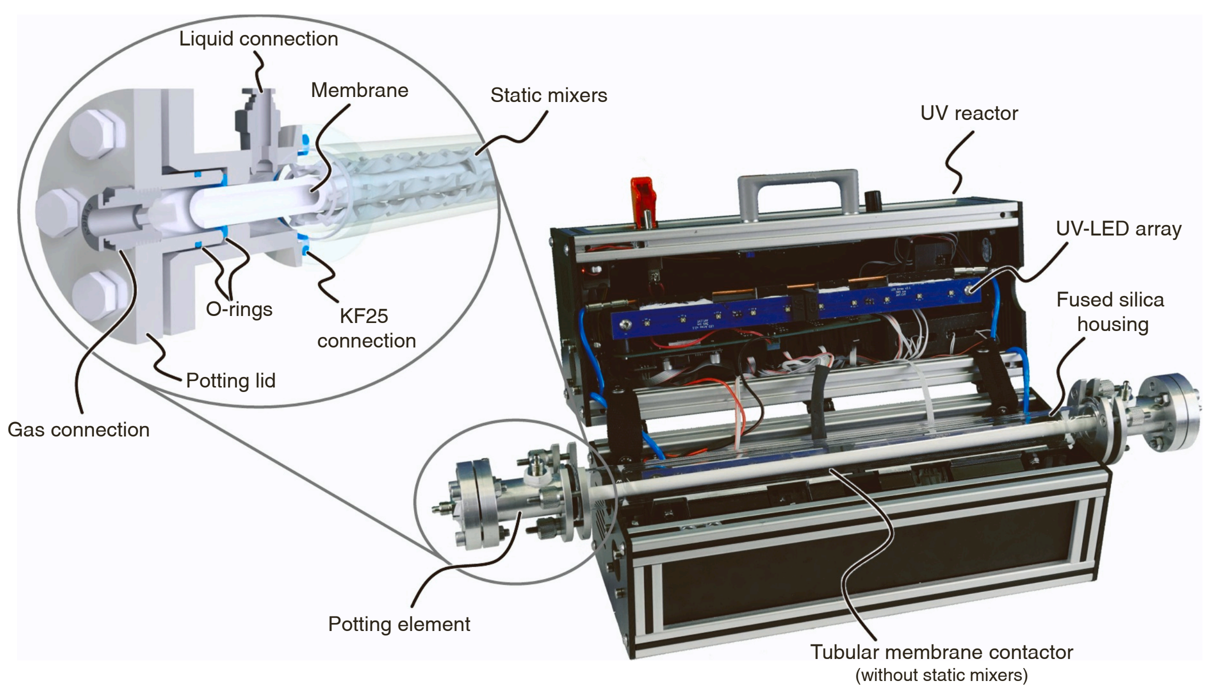

Fig. 3. Picture of the tubular membrane contactor in the opened UV reactor. The detailed rendering shows the principle of the potting element to separate the gas and liquid sides of the membrane contactor.

membrane contactor enables the gas pressure adjustment. The experiments are performed with a gas flow rate of approximately 30 L h^{-1} and a gas-side pressure of 0.35 bar. The off-gas is dehumidified in a cold trap before entering an ozone destruction unit using a manganese catalyst Carulite 200 (Lehmann & Voss & Co. KG, Germany).

Deionized (DI) water is pumped from a reservoir through the membrane contactor's shell-side using a MCP-Z process (Ismatec SA, Switzerland) gear pump with an MI0280 (Ismatec SA, Switzerland) pump head. The water flow rate is varied between 100 mL min^{-1} and 300 mL min^{-1} resulting in residence times between 60 s and 20 s, respectively. A sample valve behind the membrane contactor is used to take samples for measurements of the dissolved ozone concentration. All data points of ozonation experiments are measured at least three times. Ozonated water is collected in a second reservoir in a fume hood. All tubing in the experimental setup is made from PTFE.

For mass transfer characterization, the mass transfer coefficient K_L is calculated, according to Pines et al. [50], using the measured dissolved ozone concentration at the outlet of the membrane contactor $c_{l,out}$ with

$$K_L = \frac{\dot{V}}{A_{mem}} \cdot ln\left(\frac{c_g \cdot H_S^{cc}}{c_g \cdot H_S^{cc} - c_{l,out}}\right)$$

where $\dot{V}$ is the volume flow rate of water, A_{mem} the active membrane surface area in the membrane contactor, c_g the gaseous ozone concentration, and H_S^{cc} the Henry coefficient of ozone in water obtained from

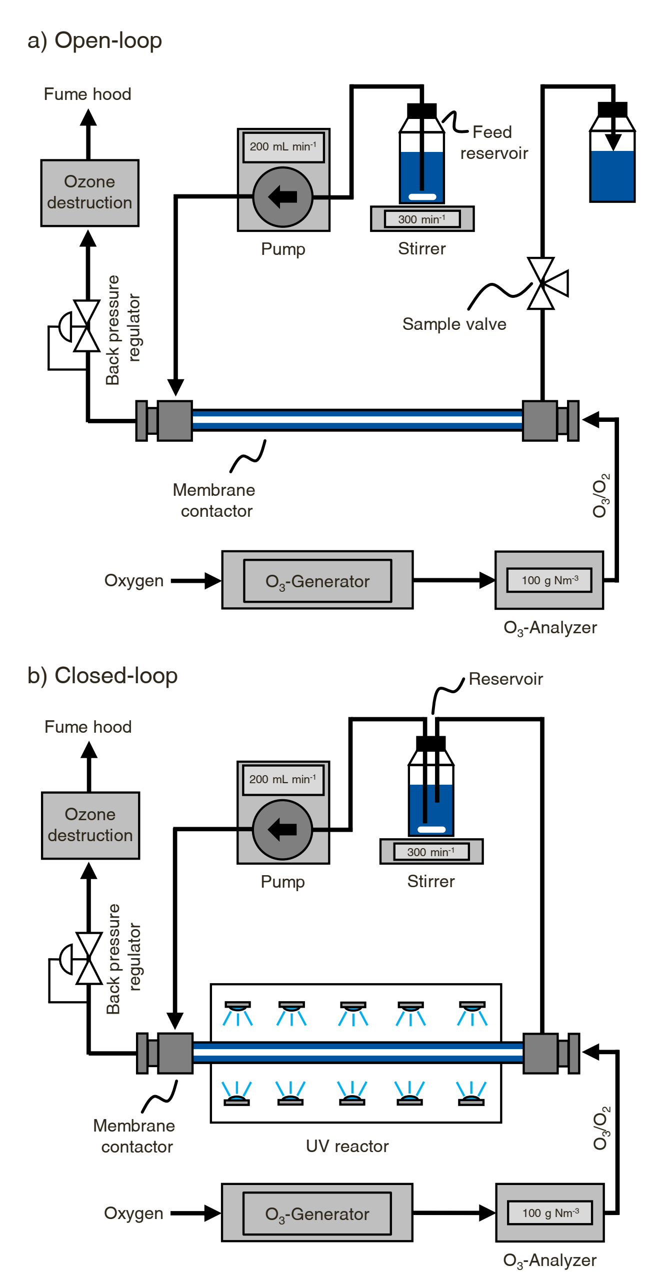

Fig. 4. Experimental setup for ozone mass transfer (a) and MP degradation (b) experiments.

Sander [51].

For MP degradation experiments, a closed-loop configuration, according to Figure 4 b), is used. The gas-side of the experimental setup is similar to the open-loop configuration. However, the liquid-side is changed to a circulation loop with one stirred reservoir filled with 1 L of MP-spiked water. Water is pumped at a flow rate of 200 mL min^{-1} through the membrane contactor. The gas-side ozone flow rate is approximately 30 L h^{-1} with a gaseous ozone concentration of 100 g N m^{-3} at a pressure of approximately 0.35 bar. Sulfamethoxazole (SMX) (Sigma-Aldrich / Merck, Germany), Carbamazepine (CBZ) (TCI Europe N.V., Belgium), Diclofenac (DCF) (Sigma-Aldrich / Merck, Germany), and Diatrizoate (DTA) (Sigma-Aldrich / Merck, Germany) are used as pharmaceutical MPs in this work. The initial cumulated MP concentration is 0.08 mmol L^{-1} for all experiments. Hence, in experiments with a matrix of four MPs, the concentration of each MP is 0.02 mmol L^{-1} to ensure equimolar conditions in all experiments. The MP-spiked stock solution is prepared with MilliQ water (Merck Millipore, United States) in a flask under stirring. Samples for high-performance liquid chromatography (HPLC) analysis with a volume of 2 mL are taken every 5 min from the stirred reservoir during the experiment. Samples for TOC analysis with a volume of 10 mL are taken every 30 min from the stirred reservoir to minimize the sample volume taken during the experiment. Overall, the sample volume during each experiment is below 10% of the total water volume. MP matrix degradation experiments and bubble-free single MP degradation experiments are repeated three times.

For photocatalytic ozonation experiments, the membrane contactor is placed in a self-made UV reactor, as shown in Figure 3. The UV reactor is equipped with 30 UV-LEDs CUN6GF1A (Seoul Viosys, Korea) with a total radiant flux of 42 W at a peak wavelength of 367 nm. The LEDs are arranged in three arrays with 10 LEDs each. The arrays are placed around the fused silica housing spaced by 120∘ to irradiate the membrane contactor from all sides. The irradiated length of the UV reactor is 300 mm. Detailed information on the UV reactor can be found in a previous publication [52]. Four static mixer elements are placed in the membrane contactor for photocatalytic ozonation experiments with static mixers.

2.4. *Analytical methods*

Water contact angles are measured with a Drop Shape Analysis System DAS 10-Mk2 (Krüss GmbH, Germany). Field emission scanning electron microscope (FESEM) pictures are taken with a SU 5000 FE-SEM (Hitachi Ltd., Japan) with a Quantax XFlash 6–60 (Bruker Corp., United States) for energy-dispersive X-ray spectroscopy (EDX), and a TM3030Plus (Hitachi Ltd., Japan) with an X-Flash MIN SVE (Bruker Corp., United States) for EDX. The dissolved ozone concentration in water is measured with cuvette tests LCK 310 (Hach Lange GmbH, Germany) and a DR 2800 photometer (Hach Lange GmbH, Germany). The concentration of MPs is analyzed with HPLC using a 1260 Infinity II using a diode-array detector (DAD) (Agilent Technologies Inc., United States). SMX, CBZ, and DCF are analyzed using a LiChrospher 100 RP-18 (Merck, Germany) column at 35 ˚C. The detection wavelength of the DAD is 265 nm for SMX and 285 nm for CBZ and DCF. DTA is analyzed using a Luna C18(2) 100A (Phenomenex, United States) column at 30 ˚C and a detection wavelength of the DAD of 238 nm. The TOC content of water samples is analyzed with a TOC-LCPH (Shimadzu Corp., Japan) using the difference method. The pH value of samples is measured with a FiveEasy F20 (Mettler Toledo Inc., United States).

3. Results and discussion

3.1. *Bubble-less ozonation*

Both coating methods, support layer coating and selective layer coating, are used to prepare hydrophobic membranes. The water contact angle is increased from 25∘ to above 115∘ by using selective layer coating. However, the coating is unstable under experimental conditions, with ozone diffusing through the membrane and water flowing on the shell-side of the membrane. Due to the lack of chemical binding of the PTFE layer to the ceramic membrane, the layer disintegrates and the membrane is wetted. FESEM pictures of coated membranes before and after an experiment are shown in the SI.

To increase the mechanical stability of the PTFE coating, the filtration direction is reversed and the PTFE particles are filtered from the lumen-side through the support layer onto the selective layer. Ozone mass transfer experiments are conducted to characterize the stable separation of water and gas phases in the membrane contactor, which is the overall aim of the hydrophobization procedure.

Figure 5 a) shows the dissolved ozone concentration in DI water as a function of the water flow rate and operation mode of the membrane contactor. In all experiments with support layer coating, no water break-

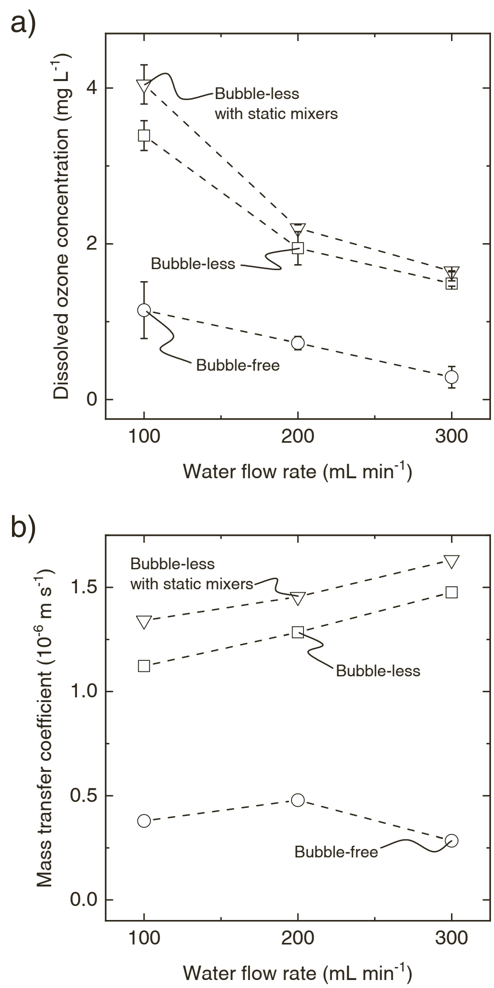

Fig. 5. Ozonation experiments with support layer coated membranes in open-loop configuration. a) Dissolved ozone concentrations in DI water at the outlet of the membrane contactor. b) Mass transfer coefficients calculated using the measured ozone concentrations.

through was observed on the gas-side of the membrane contactor. Thus, the filtration of PTFE particles on the back side of the selective layer seems sufficient to create a stable phase boundary between water and a gas mixture consisting of ozone and oxygen. Furthermore, the membranes are used for several experiments without affecting the stability of the phase boundary. Hence, the applied support layer coating is assumed to be stable.

Three operation modes are used for the ozonation experiments: bubble-free, bubble-less, and bubble-less with static mixers. Bubble-free ozonation experiments are performed with a pressure slightly below the first bubble point of the respective membrane. Thus, no bubbles are formed on the membrane's surface, and ozone mass transfer is limited to diffusive mass transport through the membrane. In bubble-less ozonation, the experiment is conducted at the first bubble point therefore a few small bubbles form at the largest pore of the membrane.

As shown in Figure 5 a), the dissolved ozone concentration at the outlet of the membrane contactor decreases with increasing water flow rate for all three operation modes due to a decreased residence time. Furthermore, the ozone concentration with bubble-less ozonation is significantly increased by up to 420% and 195% for flow rates of 300 mL min^{-1} and 100 mL min^{-1}, respectively. This is a result of two effects. First, the gas-side pressure is increased in bubble-less operation, resulting in a shifted phase boundary in the membrane towards the liquid phase. Hence, a shorter diffusive length through the wetted part of the membrane is realized, minimizing the mass transfer resistance, as shown by Janknecht et al. [53]. Second, the few ozone gas bubbles within the membrane contactor act as additional surface area for ozone mass transfer.

The implementation of static mixers into the membrane contactor further increases the dissolved ozone concentration by 10–20% for water flow rates of 300 mL min^{-1} and 100 mL min^{-1}, respectively. The increase compared to bubble-less ozonation without static mixers is most significant for low water flow rates in the membrane contactor due to a drop in Reynolds number from 200 to 65. The effect of additional radial mixing by static mixers is stronger at low Reynolds numbers compared to higher Reynolds numbers, where first self-induced radial flow components might occur due to the flow conditions. A comprehensive study on the effects of static mixers on flow conditions in the membrane contactor of this work, ozone mass transfer and micropollutant degradation can be found in a previous publication [30].

Figure 5 b) shows the calculated mass transfer coefficients for the membrane contactor at different flow rates and operation modes. While the mass transfer coefficient increases with the flow rate in bubble-less ozonation, the mass transfer coefficient decreases at high flow rates in bubble-free ozonation. This indicates a mass transfer limitation in the membrane in bubble-free ozonation at high flow rates. Thus, bubble-free ozonation with static mixers was not characterized, as the membrane already limits the mass transfer process, and further optimizing the liquid-side mass transfer resistances is ineffective. In contrast, in bubble-less ozonation, the mass transfer is limited by a lack of convective ozone mass transport from the membrane to the bulk phase. Thus, the mass transfer coefficient increases with increasing flow rate and by the addition of static mixers with all tested flow rates. Overall, the mass transfer coefficient is in the order of $0.4 \cdot 10^{-6}$ ms^{-1} for bubble-free ozonation, $1.3 \cdot 10^{-6}$ ms^{-1} for bubble-less ozonation, and $1.5 \cdot 10^{-6}$ ms^{-1} for bubble-less ozonation with static mixers, which is an increase of 14% by the addition of static mixers.

In literature, ceramic membrane contactors for ozonation are reported with mass transfer coefficients in the order of $1.1 \cdot 10^{-6}$ ms^{-1} at pH 3 by Wenten et al. [54] and $1.5 \cdot 10^{-5}$ ms^{-1} to $2.0 \cdot 10^{-5}$ ms^{-1} by Stylianou et al. [37] for ceramic membranes with a hydrophobic fluorinated silane treatment. The membrane contactor of this work is in the same order of magnitude as the membrane contactor of Wenten et al. However, the mass transfer coefficient is one order of magnitude smaller compared to Stylianou et al. This can be explained by the support layer coating used for the hydrophobic treatment in this work, compared to a selective layer coating by Stylianou et al. Furthermore, they use fluorinated silanes for the hydrophobic treatment that are in direct contact with the treated water. As these fluorinated silanes are classified as per- and polyfluoroalkyl substances (PFAS), which are persistent, bioaccumulative, and harmful to all living organisms, they might be problematic for use in a water treatment process. In contrast, the membrane contactor of this work uses inert PTFE for the hydrophobic treatment, and the PTFE particles are captured inside the membrane's structure, lowering the risk of leaching significantly.

3.2. Single micropollutant degradation

First, the concept of bubble-less photocatalytic ozonation using a membrane contactor is tested with the highly oxidizable SMX as a model MP. The first degradation experiment is done with the membrane contactor using polymeric 3D printed potting elements and static mixers. Figure 6 a) and b) show the relative SMX concentration and TOC content in water for bubble-free operation, respectively. The SMX concentration decreases for all operation modes and reaches complete SMX degradation within 90 min and 85 min for ozonation and photocatalytic ozonation, respectively. This is in accordance with literature where SMX is known as a highly oxidizable MP that can directly react with ozone and hydroxyl radicals [55,56]. When static mixers are added to the system, the time to complete degradation decreases to 60 min due to enhanced ozone mass transfer, as discussed above. The degradation rate of SMX is

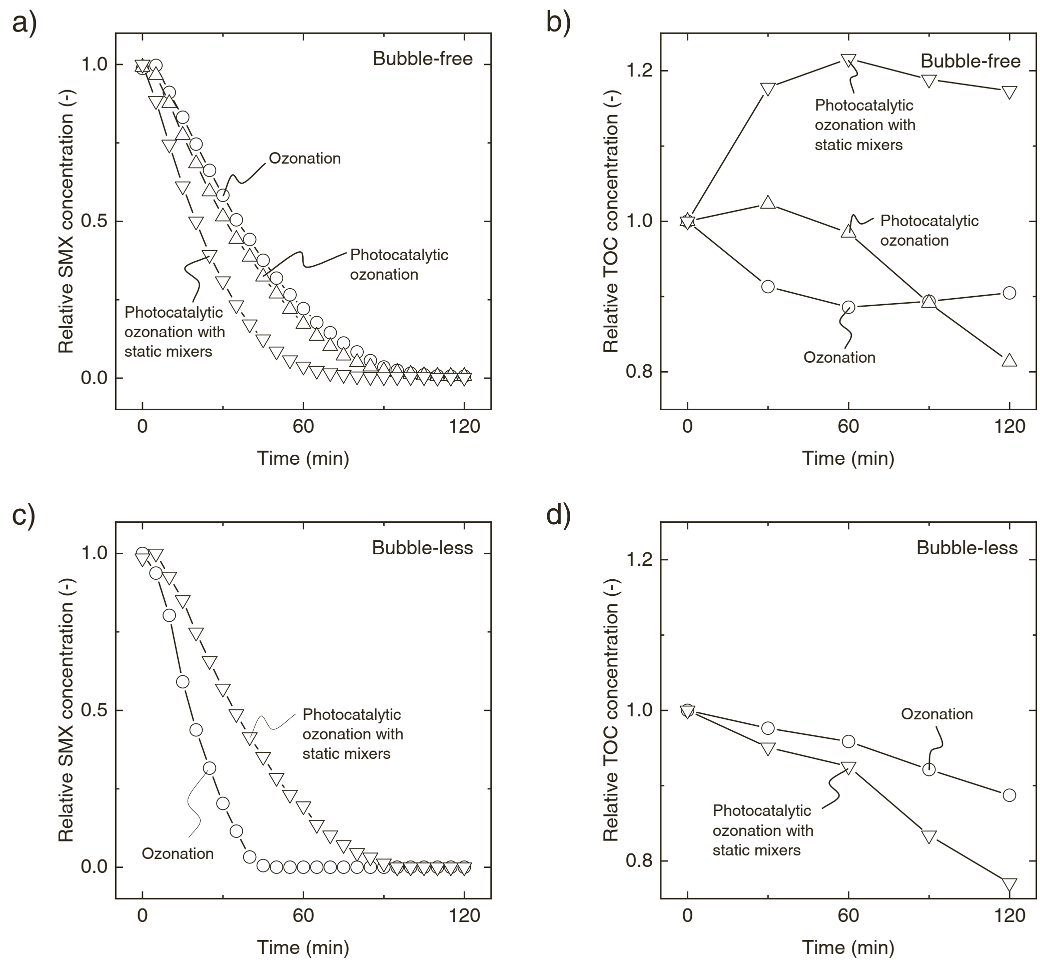

Fig. 6. Micropollutant degradation experiments with sulfamethoxazole (SMX) as model micropollutant. The start concentration of SMX is 0.08 mmol L^{-1} for all experiments. All experiments are done in a closed-loop configuration with different processes: ozonation, photocatalytic ozonation, and photocatalytic ozonation with static mixers. a) Relative SMX concentration over experimental time for bubble-free operation with polymeric static mixers. b) Relative TOC concentration over experimental time for bubble-free operation with polymeric static mixers. c) Relative SMX concentration over experimental time for bubble-less operation with aluminum static mixers. d) Relative TOC concentration over experimental time for bubble-less operation with aluminum static mixers.

not enhanced by applying additional UV light to the membrane contactor, confirming that ozone is directly degrading SMX as an increased ozone decay to hydroxyl radicals does not lead to an increased SMX degradation. Furthermore, the hydroxyl radical concentration may already be increased by the presence of TiO_2 catalyst during ozonation, as this is a catalytic ozonation process. However, the implementation of static mixers into the membrane contactor increases the SMX degradation rate, and complete degradation is achieved 33% faster compared to ozonation due to enhanced ozone mass transfer, as shown in Figure 6 a). Nevertheless, the TOC removal with ozonation is just 10% after 120 min and 20% with photocatalytic ozonation, as shown in Figure 6 b). By adding the first version of static mixers, made from polymeric 3D print resin, the TOC is not reduced but increased by up to 21% compared to the initial TOC concentration. Hence, it is concluded that the 3D printed polymer is not even short-term stable in the corrosive environment during photocatalytic ozonation. This also influences the repeatability of experiments as the progressing degradation of polymeric parts influences the SMX degradation due to increasing undesired side reactions of oxidizing species with the polymeric material. A detailed discussion can be found in the SI. The lack of material stability leads to the degradation of the polymeric static mixers and the leaching of organic molecules into the water, increasing the TOC, as shown in Figure 6 b). Thus, the static mixers are made from 3D printed aluminum for all bubble-less experiments.No degradation is observed for aluminum parts in the membrane contactor after the use in over 40 experiments.

To further increase the SMX degradation rate and TOC removal, bubble-less operation at the first bubble point of the membrane is used. The increased gaseous pressure shifts the phase boundary within the membrane material towards the water phase. However, the main ozone mass transfer mechanism is still diffusion at the membrane's surface. Bubbles form only at the largest pore of the membrane and the total bubble surface area is below 2% of the membrane's surface area. The results for bubble-less operation with aluminum static mixers are presented in Figure 6 c) and d). The complete degradation with sole ozonation is achieved after just 45 min, which is a decrease of 50% compared to bubble-free operation, due to a higher ozone concentration and a higher ozone availability for reactions with SMX molecules as no other reactions, i.e., with polymeric parts of the reactor, are possible. Over the course of the experiment, the pH value drops from 7.1 to 4.1. Thus, the natural ozone decay is increasingly suppressed over time.

The TOC decreases over time for ozonation and photocatalytic ozonation with static mixers in bubble-less experiments with aluminum static mixers, as shown in Figure 6 d). This indicates that no undesired side reactions and degradation of the static mixer material occur, explaining the significantly improved TOC removal of photocatalytic ozonation with static mixers compared to Figure 6 b). The TOC concentration gradient, shown in Figure 6 d), is higher for photocatalytic ozonation with static mixers compared to sole ozonation. This explains the slower initial SMX degradation as more parallel reactions of SMX degradation products with ozone and hydroxyl radicals take place, and less of these oxidizing species are available for initial SMX degradation. Furthermore, the TOC concentration gradient increases for both processes after 60 min, when all initial SMX molecules are degraded to smaller molecules and all oxidizing species are available for further mineralization reactions. The photocatalytic ozonation with static mixers results in a 109% higher TOC removal after 120 min compared to sole ozonation, as shown in Figure 6 d).

Despite the enhanced ozone mass transfer and radial mixing in the membrane contactor, the implementation of static mixers also has a drawback for photocatalytic ozonation. The static mixers produce shadows on the membrane; thus, the photon efficiency of the photocatalytic process is decreased. To minimize shadows on the membrane, just six static mixers are arranged around the membrane with a certain distance between the static mixers. This allows UV light to reach large parts of the membrane unhindered, while it decreases the mixing efficiency due to the distance between the static mixers. This trade-off was not optimized within this work. However, the reactor design for high photon efficiencies with even light distribution becomes essential for further optimization and upscaling the membrane-based bubble-less photocatalytic ozonation. [57,58]

Furthermore, experiments with the single micropollutant CBZ are conducted, and Figures 7 a) and b) show the relative CBZ concentration for bubble-free and bubble-less operation of the membrane contactor. CBZ degradation experiments start with a pH of 5.7 that drops to 4.2 after 120 min. The CBZ degradation significantly increases using photocatalytic ozonation with static mixers compared to sole ozonation in bubble-free operation. This indicates CBZ degradation benefits from increased hydroxyl radical concentration and increased mixing when the process is mass transfer limited due to bubble-free operation. An overall increase in mass transfer by using bubble-less operation significantly decreases the time to complete CBZ degradation by 65% for ozonation and 44% for photocatalytic ozonation with static mixers, as shown in Figures 7 a) and b). However, in bubble-less ozonation, the degradation rate does not increase with photocatalytic ozonation with static mixers. The degradation rate limitation observed in bubble-free ozonation is already overcome in bubble-less ozonation due to an overall increased ozone mass transfer. Nevertheless, the relative TOC concentration, shown in Figure 7 c), reveals an advantage of the photocatalytic ozonation with static mixers as the TOC concentration decreases faster compared to sole ozonation. After 120 min, 41% TOC removal is observed for photocatalytic ozonation with static mixers and just 23% for ozonation. Thus, the TOC removal is increased by 78% by using the photocatalytic process with static mixers. Similar to the SMX experiments, the increased reactions of oxidizing species with CBZ degradation products, shown by the increased TOC removal, can explain the slightly slower decrease in CBZ concentration for photocatalytic ozonation with static mixers compared to ozonation.

Overall, experiments with single MPs reveal that polymeric materials are not suitable for the process due to a lack of stability against the oxidizing species, and all parts need to be manufactured from either aluminum or PTFE. Furthermore, the bubble-less operation is advantageous compared to bubble-free ozonation due to higher ozone mass transfer, while the primary ozone mass transfer mechanism is still a membrane contactor. Thus, all further experiments are conducted with bubble-less operation.

3.3. Micropollutant matrix degradation

After preliminary experiments with single MPs in water, the experimental setup is changed to a matrix of four different MPs to represent more lifelike conditions with several parallel reactions. Figure 8 shows the degradation of SMX, DCF, DTA, and CBZ in experiments where all four MPs are present in the water matrix simultaneously. Bubble-less operation of the membrane contactor is used for all experiments. The pH value of the water matrix starts at 7.0 for all operation modes and drops down to 3.7, 4.0, and 3.7 for sole ozonation, photocatalytic ozonation, and photocatalytic ozonation with static mixers, respectively. The concentration gradients are very similar for SMX, DCF, and CBZ, while the degradation of DTA is slower and does not achieve complete degradation within 120 min. DTA as an ionic X-ray contrast agent is reported in the literature as very stable in ozonation processes [15,18]. Thus, significantly lower degradation of DTA is expected. Overall, the results of the matrix experiments are in accordance with results from single MP experiments. Furthermore, in matrix experiments, the MP degradation becomes faster from ozonation to photocatalytic ozonation with static mixers for all four MPs, in contrast to single MP experiments where ozonation yielded faster MP degradation in bubble-less operation. However, the differences in degradation rate are very small for SMX, DCF, and CBZ. In contrast, DTA degradation significantly benefits from photocatalytic ozonation and the addition of static mixers. Complete degradation is achieved after 35 min, 30 min, and 35 min for SMX, DCF, and CBZ, respectively, using photocatalytic ozonation with static mixers. This is an advantage of 36%, 33%, and 30% for SMX, DCF, and CBZ, respectively, compared to ozonation. Furthermore, the degradation of DTA increases by 24% with photocatalytic ozonation and by 37% with additional static mixers, compared to ozonation. A DTA degradation of 88% is observed after 120 min using photocatalytic ozonation with static mixers.

DTA degradation using ozone in real wastewater is reported by Ternes et al. [59] with a maximum DTA degradation of 14% at an initial DTA concentration of 9 nmol L^{-1} and an ozone dose of 15 mg L^{-1}. For ozone doses between 1 mg L^{-1} and 5 mg L^{-1}, no degradation was

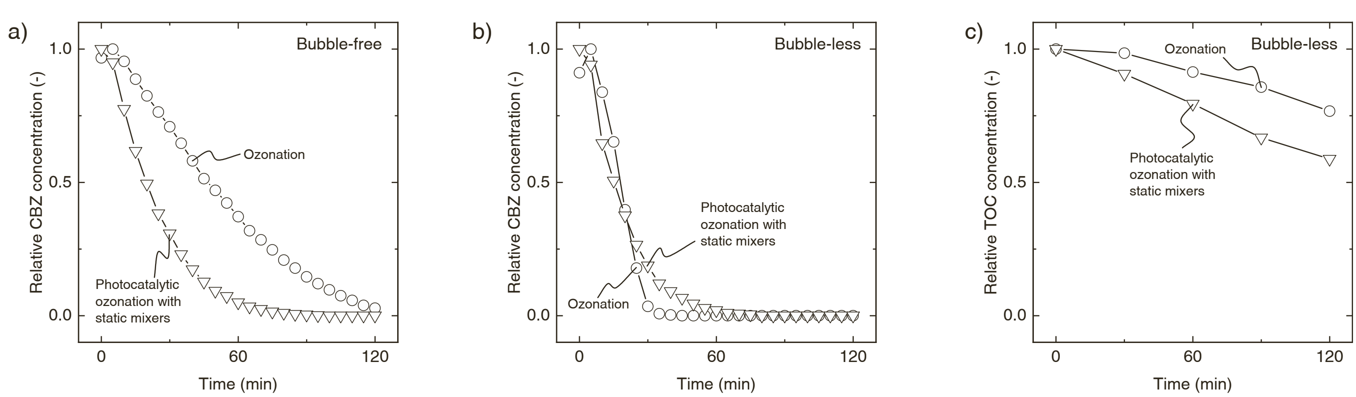

Fig. 7. Micropollutant degradation experiments with carbamazepine (CBZ) as a model micropollutant. The start concentration of CBZ is 0.08 mmol L^{-1} for all experiments. All experiments are done in a closed-loop configuration with different processes: ozonation, photocatalytic ozonation, and photocatalytic ozonation with static mixers. a) Relative CBZ concentration over experimental time for bubble-free operation. b) Relative CBZ concentration over experimental time for bubble-less operation. c) Relative TOC concentration over experimental time for bubble-less operation.

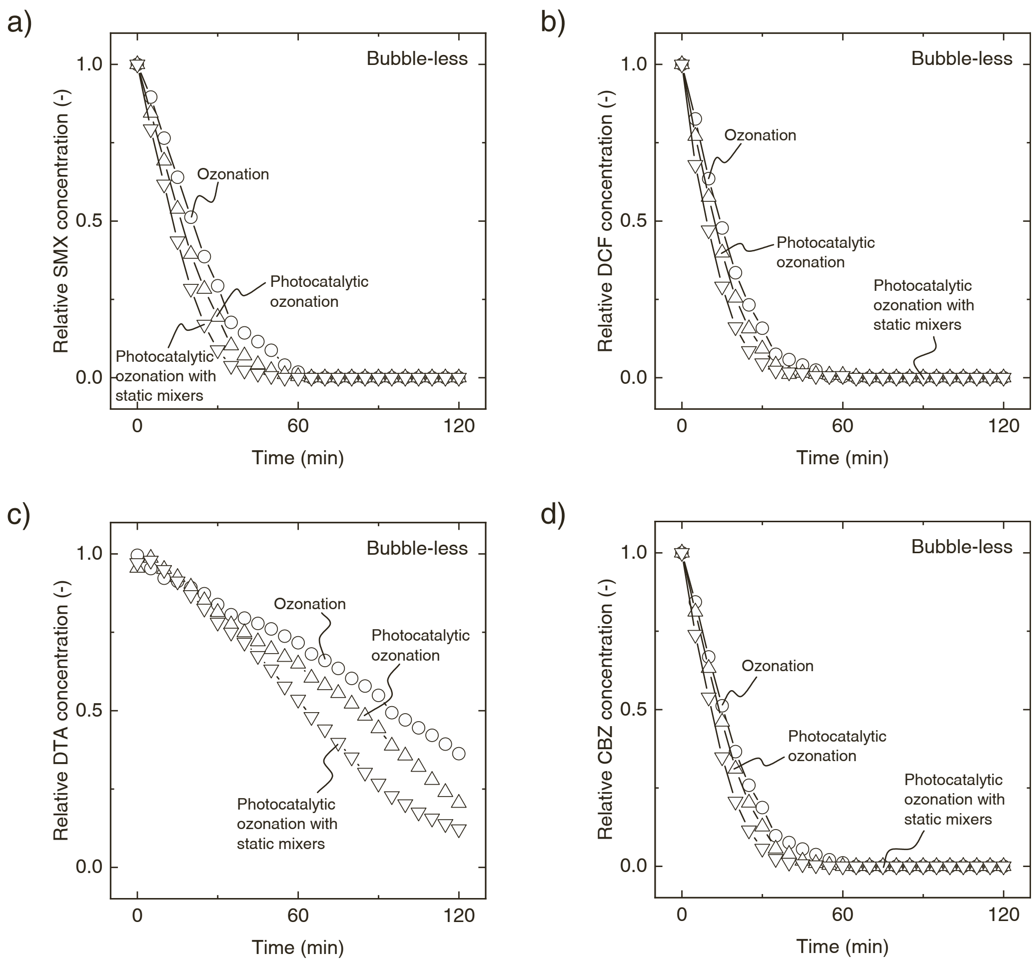

Fig. 8. Relative MP concentration over experimental time for degradation experiments with a micropollutant matrix of SMX, DCF, DTA, and CBZ with an overall start concentration of 0.08 mmol L^{-1} in closed-loop configuration with bubble-less operation. a) Relative SMX concentration. b) Relative DCF concentration. c) Relative DTA concentration. d) Relative CBZ concentration.

observed by Ternes et al. and Huber et al. [59,60] with an initial DTA concentration of 9 nmol L^{-1} and 8.0 nmol L^{-1}, respectively. Sugihara et al. [61] studied photocatalytic DTA degradation using suspended TiO_2 catalyst with UV-A radiation. Under lab conditions with an initial DTA concentration of 20 μmol L^{-1}, they observed a DTA degradation of 65% - 70% within 60 min. Radjenovic et al. [62] studied electrochemical reduction and oxidation of DTA with an initial concentration of 5 μmol L^{-1} and 50 μmol L^{-1} DTA. Their results show 80% - 90% DTA removal using electrochemical reduction with Pd-loaded graphite felts as cathode material under lab conditions. The DTA removal dropped to 50% - 60% after 3 h for hospital wastewater. Combined oxidation and reduction experiments using a boron-doped diamond anode with the Pd-loaded graphite felt cathode revealed complete degradation of DTA within 2 h under lab conditions and 60% degradation for hospital wastewater. However, the electrochemical treatment requires very expensive electrode materials and the addition of an electrolyte for efficient DTA degradation. An alternative method to remove DTA from wastewater is adsorption on activated carbon. Landwehrkamp et al. [63] studied DTA removal with an initial concentration of 16 nmol L^{-1} and reported a removal efficiency between 63% and 83% on different activated carbons. However, using this method, DTA is not degraded, but contaminated adsorbent waste is generated.

Hence, the bubble-less photocatalytic ozonation process of this work seems superior to current advanced treatment processes for the degradation of iodinated X-ray contrast agent as the degradation is increased by 530% compared to sole ozonation and by 25% compared to photocatalytic degradation reported in the literature. Furthermore, bubble-less photocatalytic ozonation reaches a higher removal efficiency than adsorption on activated carbon and approximately the same removal efficiency as electrochemical oxidation and reduction. Nevertheless, bubble-less photocatalytic ozonation avoids drawbacks like the necessity for expensive electrode materials or the generation of contaminated waste.

The superior performance of photocatalytic ozonation using the membrane contactor of this work relies on two mechanisms. First, the increased concentration of oxidizing species, e.g., hydroxyl radicals, $O_3^{\bullet-}$, $O_2^{\bullet-}$, generated at the photocatalyst and due to accelerated ozone decay to these oxidizing species at the photocatalyst increases MP degradation [24]. In contrast to dissolved ozone, these oxidizing species react non-selectively with organic molecules and can degrade MPs that are stable in conventional ozonation, e.g., DTA. Second, enhanced mixing with static mixers ensures a homogeneous distribution of oxidizing species throughout the whole reactor volume, increasing their availability for degradation reactions [30]. Thus, MP degradation is not limited to a small volume around the membrane contactor or ozone bubbles, as in conventional ozonation, resulting in a higher MP degradation. These two mechanisms of bubble-less photocatalytic ozonation with static mixers not only enhance MP degradation but also significantly enhance TOC removal.

Figure 9 shows the corresponding relative TOC concentration during matrix experiments. The TOC removal increases by 94% using photocatalytic ozonation and by 115% using additional static mixers in the

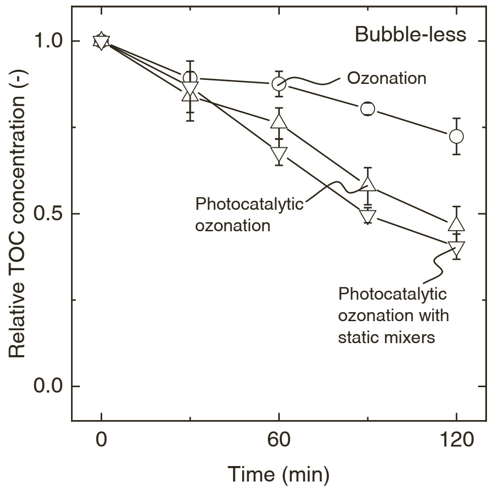

Fig. 9. Relative TOC concentration over experimental time for degradation experiments with a micropollutant matrix of SMX, DCF, DTA, and CBZ with an overall start concentration of 0.08 mmol L^{-1} in closed-loop configuration with bubble-less operation.

membrane contactor compared to ozonation. The photocatalytic ozonation with static mixers achieves a TOC removal of 60% within 120 min. The small standard deviation represented by the error bars in Figure 9 indicate reasonable repeatability of MP matrix experiments. However, the standard deviations in degradation of the four individual MPs, as shown in Figure S6 of the SI, are higher than the cumulated deviation in TOC removal as the sum parameter of all parallel degradation reactions. This indicates a competition for oxidizing species between several parallel reaction pathways, affecting the repeatability. A detailed discussion on this is presented in the SI. Overall, the MP matrix experiments reveal the significant advantages of photocatalytic ozonation with the addition of static mixers with respect to the MP degradation rate and TOC removal.

4. Conclusion

A tubular lab-scale membrane contactor for photocatalytic ozonation is designed in this work. A viable method for hydrophobic treatment of a tubular ceramic membrane is established. Filtration of PTFE particles into the support layer of the ceramic membrane enables the use of intrinsically hydrophilic ceramic membranes for a stable phase separation between gaseous ozone and water without flooding the membrane.

Mass transfer experiments show that ozonation is possible with hydrophobic treated ceramic membranes in bubble-free and bubble-less operation. However, the mass transfer coefficient is significantly higher with bubble-less ozonation with values of $1.3 \cdot 10^{-6}$ m s^{-1} for bubble-less ozonation, and $0.4 \cdot 10^{-6}$ m s^{-1} for bubble-free ozonation. Further improvements in mass transfer are achieved by implementing circular-arranged static mixers. The mass transfer coefficient of the membrane contactor is increased by 14% by adding static mixers.

The degradation of MPs using the membrane contactor for photocatalytic ozonation reveals a significant improvement in TOC removal of 94% compared to ozonation. The TOC removal can be even further improved by the implementation of static mixers, resulting in a 115% increased TOC removal compared to ozonation. Furthermore, the degradation of all four investigated MPs is accelerated using photocatalytic ozonation with static mixers. The most significant effect is observed for the iodinated X-ray contrast agent DTA. An 88% DTA degradation is observed after 120 min by photocatalytic ozonation with static mixers.

For future work, we aim to increase the TiO_2 covered surface area within the reactor to enhance the degradation of MPs further. For this, static mixers can be 3D printed from titanium, and electrochemical oxidation can create a thin TiO_2 surface layer. This process has already been demonstrated in the literature, e.g., by Gomes et al. [64], for photocatalytic processes. A subsequent heat treatment at 450 ˚C changes the morphology of TiO_2 from amorphous to an anatase crystal structure. Thus, the static mixers themselves act as additional photocatalytic surfaces for MP degradation.

CRediT authorship contribution statement

Stefan Herrmann: Writing – review & editing, Writing – original draft, Visualization, Methodology, Investigation, Conceptualization. **Konstantin Dietz:** Writing – original draft, Validation, Investigation. **Lennart Wilms:** Writing – original draft, Validation, Investigation. **Matthias Wessling:** Writing – review & editing, Project administration, Funding acquisition, Conceptualization.

Declaration of Competing Interest

The authors declare that they have no known competing financial interests or personal relationships that could have appeared to influence the work reported in this paper.

Data Availability

Data will be made available on request.

Acknowledgments

M.W. acknowledges DFG funding through the Gottfried Wilhelm Leibniz Award 2019 (WE 4678/12-1). The authors thank Timo Linzenmeier, Justin Gottfried, and Frederike Schiszler for the analysis of a large amount of HPLC samples, and Karin Faensen for FESEM pictures.

Appendix A. Supporting information

Supplementary data associated with this article can be found in the online version at doi:10.1016/j.jece.2024.112995.

References

[1] N.M. Kumar, M.C. Sudha, T. Damodharam, S. Varjani, Micro-Pollutants in Surface Water: Impacts on the Aquatic Environment and Treatment Technologies (Current Developments in Biotechnology and Bioengineering), Elsevier, 2020, pp. 41–62, https://doi.org/10.1016/B978-0-12-819594-9.00003-6 (Current Developments in Biotechnology and Bioengineering).
[2] C.L. SpindolaVilela, T.L. Damasceno, T. Thomas, R.S. Peixoto, Global qualitative and quantitative distribution of micropollutants in the deep sea, Environ. Pollut. 307 (2022) 119414, https://doi.org/10.1016/j.envpol.2022.119414.
[3] P. Bhatt, G. Bhandari, M. Bilal, Occurrence, toxicity impacts and mitigation of emerging micropollutants in the aquatic environments: recent tendencies and perspectives, J. Environ. Chem. Eng. 10 (3) (2022) 107598, https://doi.org/10.1016/j.jece.2022.107598.
[4] T. Eregowda, S. Mohapatra, Fate of micropollutants in engineered and natural environment, in: M. Kumar, F. Munoz-Arriola, H. Furumai, T. Chaminda (Eds.), Resilience, Response, and Risk in Water Systems, Springer Transactions in Civil and Environmental Engineering, Springer, Singapore, Singapore, 2020, pp. 283–301, https://doi.org/10.1007/978-981-15-4668-6.
[5] Y. Shao, Z. Chen, H. Hollert, S. Zhou, B. Deutschmann, T.-B. Seiler, Toxicity of 10 organic micropollutants and their mixture: Implications for aquatic risk assessment, Sci. Total Environ. 666 (2019) 1273–1282, https://doi.org/10.1016/j.scitotenv.2019.02.047.
[6] C. Grandclément, I. Seyssiecq, A. Piram, P. Wong-Wah-Chung, G. Vanot, N. Tiliacos, N. Roche, P. Doumenq, From the conventional biological wastewater treatment to hybrid processes, the evaluation of organic micropollutant removal: a review, Water Res. 111 (2017) 297–317, https://doi.org/10.1016/j.watres.2017.01.005.
[7] M. Abily, V. Acuña, L. Corominas, I. Rodríguez-Roda, W. Gernjak, Strategic routes for wastewater treatment plant upgrades to reduce micropollutants in european surface water bodies, J. Clean. Prod. 415 (2023) 137867, https://doi.org/10.1016/j.jclepro.2023.137867.
[8] E.Y. Klein, T.P. van Boeckel, E.M. Martinez, S. Pant, S. Gandra, S.A. Levin, H. Goossens, R. Laxminarayan, Global increase and geographic convergence in

antibiotic consumption between 2000 and 2015, Proc. Natl. Acad. Sci. USA 115 (15) (2018) E3463–E3470, https://doi.org/10.1073/pnas.1717295115.
[9] O.I. GonzálezPeña, M.Á. LópezZavala, H. CabralRuelas, Pharmaceuticals market, consumption trends and disease incidence are not driving the pharmaceutical research on water and wastewater, Int. J. Environ. Res. Public Health 18 (5) (2021), https://doi.org/10.3390/ijerph18052532.
[10] O.F.S. Khasawneh, P. Palaniandy, Occurrence and removal of pharmaceuticals in wastewater treatment plants, Process Saf. Environ. Prot. 150 (2021) 532–556, https://doi.org/10.1016/j.psep.2021.04.045.
[11] S.-H. Lee, K.-H. Kim, M. Lee, B.-D. Lee, Detection status and removal characteristics of pharmaceuticals in wastewater treatment effluent, J. Water Process Eng. 31 (2019) 100828, https://doi.org/10.1016/j.jwpe.2019.100828.
[12] A. Sengar, A. Vijayanandan, Comprehensive review on iodinated x-ray contrast media: Complete fate, occurrence, and formation of disinfection byproducts, Sci. Total Environ. 769 (2021) 144846, https://doi.org/10.1016/j.scitotenv.2020.144846.
[13] L. Kovalova, H. Siegrist, U. vonGunten, J. Eugster, M. Hagenbuch, A. Wittmer, R. Moser, C.S. McArdell, Elimination of micropollutants during post-treatment of hospital wastewater with powdered activated carbon, ozone, and uv, Environ. Sci. Technol. 47 (14) (2013) 7899–7908, https://doi.org/10.1021/es400708w.
[14] M. Hou, X. Li, Y. Fu, L. Wang, D. Lin, Z. Wang, Degradation of iodinated x-ray contrast media by advanced oxidation processes: A literature review with a focus on degradation pathways, Chin. Chem. Lett. 34 (4) (2023) 107723, https://doi.org/10.1016/j.cclet.2022.08.003.
[15] J. Jeong, J. Jung, W.J. Cooper, W. Song, Degradation mechanisms and kinetic studies for the treatment of x-ray contrast media compounds by advanced oxidation/reduction processes, Water Res. 44 (15) (2010) 4391–4398, https://doi.org/10.1016/j.watres.2010.05.054.
[16] S. Lim, J.L. Shi, U. vonGunten, D.L. McCurry, Ozonation of organic compounds in water and wastewater: A critical review, Water Res. 213 (2022) 118053, https://doi.org/10.1016/j.watres.2022.118053.
[17] D. Kanakaraju, B.D. Glass, M. Oelgemöller, Advanced oxidation process-mediated removal of pharmaceuticals from water: A review, J. Environ. Manag. 219 (2018) 189–207, https://doi.org/10.1016/j.jenvman.2018.04.103.
[18] K. Ikehata, N. Jodeiri Naghashkar, M. Gamal El-Din, Degradation of aqueous pharmaceuticals by ozonation and advanced oxidation processes: A review, Ozone.: Sci. Eng. 28 (6) (2006) 353–414, https://doi.org/10.1080/01919510600985937.
[19] C. von Sonntag, U. von Gunten, Chemistry of Ozone in Water and Wastewater Treatment: From Basic Principles to Applications, IWA Publishing, 2012, https://doi.org/10.2166/9781780400839.
[20] A.M. Gorito, J.F. Pesqueira, N.F. Moreira, A.R. Ribeiro, M.F.R. Pereira, O.C. Nunes, C.M.R. Almeida, A.M. Silva, Ozone-based water treatment (o3, o3/uv, o3/h2o2) for removal of organic micropollutants, bacteria inactivation and regrowth prevention, J. Environ. Chem. Eng. 9 (4) (2021) 105315, https://doi.org/10.1016/j.jece.2021.105315.
[21] T. Merle, W. Pronk, U. vonGunten, Membro 3 x, a novel combination of a membrane contactor with advanced oxidation (o 3 /h 2 o 2) for simultaneous micropollutant abatement and bromate minimization, Environ. Sci. Technol. Lett. 4 (5) (2017) 180–185, https://doi.org/10.1021/acs.estlett.7b00061.
[22] E. Issaka, J.N.-O. Amu-Darko, S. Yakubu, F.O. Fapohunda, N. Ali, M. Bilal, Advanced catalytic ozonation for degradation of pharmaceutical pollutants-a review, Chemosphere 289 (2022) 133208, https://doi.org/10.1016/j.chemosphere.2021.133208.
[23] F. Beltran, F. Rivas, R. Monterodeespinosa, A tio2/al2o3 catalyst to improve the ozonation of oxalic acid in water, Appl. Catal. B: Environ. 47 (2) (2004) 101–109, https://doi.org/10.1016/j.apcatb.2003.07.007.
[24] M. Mehrjouei, S. Müller, D. Möller, A review on photocatalytic ozonation used for the treatment of water and wastewater, Chem. Eng. J. 263 (2015) 209–219, https://doi.org/10.1016/j.cej.2014.10.112.
[25] P.H. Presumido, R. Montes, J.B. Quintana, R. Rodil, M. Feliciano, G.L. Puma, A. I. Gomes, V.J. Vilar, Ozone membrane contactor to intensify gas/liquid mass transfer and contaminants of emerging concern oxidation, J. Environ. Chem. Eng. 10 (6) (2022) 108671, https://doi.org/10.1016/j.jece.2022.108671.
[26] A. Fernandes, M. Gagol, P. Makoś, J.A. Khan, G. Boczkaj, Integrated photocatalytic advanced oxidation system (tio2/uv/o3/h2o2) for degradation of volatile organic compounds, Sep. Purif. Technol. 224 (2019) 1–14, https://doi.org/10.1016/j.seppur.2019.05.012.
[27] M.N. Chong, B. Jin, C.W.K. Chow, C. Saint, Recent developments in photocatalytic water treatment technology: a review, Water Res. 44 (10) (2010) 2997–3027, https://doi.org/10.1016/j.watres.2010.02.039.
[28] F. Parrino, G. Camera-Roda, V. Loddo, V. Augugliaro, L. Palmisano, Photocatalytic ozonation: Maximization of the reaction rate and control of undesired by-products, Appl. Catal. B: Environ. 178 (2015) 37–43, https://doi.org/10.1016/j.apcatb.2014.10.081.
[29] R. Joshi, T. Ratpukdi, K. Knutson, A. Bhatnagar, E. Khan, Bromate formation control by enhanced ozonation: A critical review, Crit. Rev. Environ. Sci. Technol. 52 (7) (2022) 1154–1198, https://doi.org/10.1080/10643389.2020.1850169.
[30] S. Herrmann, M.C. Padligur, C.J. Bieneck, M. Wessling, Modeling of tubular membrane contactors for ozonation of water reveals reduced bromate formation with static mixers, Chem. Eng. Sci. 291 (2024) 119924, https://doi.org/10.1016/j.ces.2024.119924.
[31] M. Bourgin, B. Beck, M. Boehler, E. Borowska, J. Fleiner, E. Salhi, R. Teichler, U. vonGunten, H. Siegrist, C.S. McArdell, Evaluation of a full-scale wastewater treatment plant upgraded with ozonation and biological post-treatments: Abatement of micropollutants, formation of transformation products and oxidation by-products, Water Res. 129 (2018) 486–498, https://doi.org/10.1016/j.watres.2017.10.036.
[32] M. Ekblad, R. Juárez, P. Falås, K. Bester, M. Hagman, M. Cimbritz, Influence of operational conditions and wastewater properties on the removal of organic micropollutants through ozonation, J. Environ. Manag. 286 (2021) 112205, https://doi.org/10.1016/j.jenvman.2021.112205.
[33] K.V. Plakas, V.C. Sarasidis, S.I. Patsios, D.A. Lambropoulou, A.J. Karabelas, Novel pilot scale continuous photocatalytic membrane reactor for removal of organic micropollutants from water, Chem. Eng. J. 304 (2016) 335–343, https://doi.org/10.1016/j.cej.2016.06.075.
[34] S. Leong, A. Razmjou, K. Wang, K. Hapgood, X. Zhang, H. Wang, Tio2 based photocatalytic membranes: A review, J. Membr. Sci. 472 (2014) 167–184, https://doi.org/10.1016/j.memsci.2014.08.016.
[35] S.A. Heredia Deba, B.A. Wols, D.R. Yntema, R.G. Lammertink, Transport and surface reaction model of a photocatalytic membrane during the radical filtration of methylene blue, Chem. Eng. Sci. 254 (2022) 117617, https://doi.org/10.1016/j.ces.2022.117617.
[36] E. Bein, I. Zucker, J.E. Drewes, U. Hübner, Ozone membrane contactors for water and wastewater treatment: A critical review on materials selection, mass transfer and process design, Chem. Eng. J. 413 (2021) 127393, https://doi.org/10.1016/j.cej.2020.127393.
[37] S.K. Stylianou, K. Szymanska, I.A. Katsoyiannis, A.I. Zouboulis, Novel water treatment processes based on hybrid membrane-ozonation systems: A novel ceramic membrane contactor for bubbleless ozonation of emerging micropollutants, J. Chem. 2015 (2015) 1–12, https://doi.org/10.1155/2015/214927.
[38] S.K. Stylianou, S.D. Sklari, D. Zamboulis, V.T. Zaspalis, A.I. Zouboulis, Development of bubble-less ozonation and membrane filtration process for the treatment of contaminated water, J. Membr. Sci. 492 (2015) 40–47, https://doi.org/10.1016/j.memsci.2015.05.036.
[39] P. Janknecht, P.A. Wilderer, C. Picard, A. Larbot, Ozone–water contacting by ceramic membranes, Sep. Purif. Technol. 25 (1-3) (2001) 341–346, https://doi.org/10.1016/S1383-5866(01)00061-2.
[40] S.K. Hubadillah, Z.S. Tai, M.H.D. Othman, Z. Harun, M.R. Jamalludin, M. A. Rahman, J. Jaafar, A.F. Ismail, Hydrophobic ceramic membrane for membrane distillation: A mini review on preparation, characterization, and applications, Sep. Purif. Technol. 217 (2019) 71–84, https://doi.org/10.1016/j.seppur.2019.02.014.
[41] M. Khemakhem, S. Khemakhem, R.B. Amar, Surface modification of microfiltration ceramic membrane by fluoroalkylsilane, Desalin. Water Treat. 52 (7-9) (2014) 1786–1791, https://doi.org/10.1080/19443994.2013.807023.
[42] P. Xu, Z. Jin, T. Zhang, X. Chen, M. Qiu, Y. Fan, Fabrication of a ceramic membrane with antifouling ptfe coating for gas-absorption desulfurization, Ind. Eng. Chem. Res. 60 (6) (2021) 2492–2500, https://doi.org/10.1021/acs.iecr.1c00338.
[43] A. Aguinaco, F.J. Beltrán, J.F. García-Araya, A. Oropesa, Photocatalytic ozonation to remove the pharmaceutical diclofenac from water: Influence of variables, Chem. Eng. J. 189-190 (2012) 275–282, https://doi.org/10.1016/j.cej.2012.02.072.
[44] F.J. Beltrán, A. Aguinaco, J.F. García-Araya, Mechanism and kinetics of sulfamethoxazole photocatalytic ozonation in water, Water Res. 43 (5) (2009) 1359–1369, https://doi.org/10.1016/j.watres.2008.12.015.
[45] O. Gimeno, F.J. Rivas, F.J. Beltrán, M. Carbajo, Photocatalytic ozonation of winery wastewaters, J. Agric. Food Chem. 55 (24) (2007) 9944–9950, https://doi.org/10.1021/jf072167i.
[46] M.J. Farré, M.I. Franch, S. Malato, J.A. Ayllón, J. Peral, X. Doménech, Degradation of some biorecalcitrant pesticides by homogeneous and heterogeneous photocatalytic ozonation, Chemosphere 58 (8) (2005) 1127–1133, https://doi.org/10.1016/j.chemosphere.2004.09.064.
[47] E.M. Rodríguez, A. Rey, E. Mena, F.J. Beltrán, Application of solar photocatalytic ozonation in water treatment using supported tio2, Appl. Catal. B: Environ. 254 (2019) 237–245, https://doi.org/10.1016/j.apcatb.2019.04.095.
[48] N.F.F. Moreira, J.M. Sousa, G. Macedo, A.R. Ribeiro, L. Barreiros, M. Pedrosa, J. L. Faria, M.F.R. Pereira, S. Castro-Silva, M.A. Segundo, C.M. Manaia, O.C. Nunes, A.M.T. Silva, Photocatalytic ozonation of urban wastewater and surface water using immobilized tio2 with leds: Micropollutants, antibiotic resistance genes and estrogenic activity, Water Res. 94 (2016) 10–22, https://doi.org/10.1016/j.watres.2016.02.003.
[49] X. He, R. Chen, X. Zhu, Q. Liao, L. An, X. Cheng, L. Li, Optofluidics-based membrane microreactor for wastewater treatment by photocatalytic ozonation, Ind. Eng. Chem. Res. 55 (31) (2016) 8627–8635, https://doi.org/10.1021/acs.iecr.6b00562.
[50] D.S. Pines, K.-N. Min, S.J. Ergas, D.A. Reckhow, Investigation of an ozone membrane contactor system, Ozone.: Sci. Eng. 27 (3) (2005) 209–217, https://doi.org/10.1080/01919510590945750.
[51] R. Sander, Compilation of henry's law constants (version 5.0.0) for water as solvent, Atmos. Chem. Phys. 23 (19) (2023) 10901–12440, https://doi.org/10.5194/acp-23-10901-2023.
[52] S. Herrmann, L.T. Hirschwald, K.H. Heidmann, J. Linkhorst, M. Wessling, Lab-scale tubular led uv reactor for continuous photocatalysis, HardwareX 17 (2024) e00506, https://doi.org/10.1016/j.ohx.2023.e00506.
[53] P. Janknecht, P.A. Wilderer, C. Picard, A. Larbot, J. Sarrazin, Investigations on ozone contacting by ceramic membranes, Ozone.: Sci. Eng. 22 (4) (2000) 379–392, https://doi.org/10.1080/01919510009408782.
[54] I.G. Wenten, H. Julian, N.T. Panjaitan, Ozonation through ceramic membrane contactor for iodide oxidation during iodine recovery from brine water, Desalination 306 (2012) 29–34, https://doi.org/10.1016/j.desal.2012.08.032.
[55] B. Mathon, M. Coquery, Z. Liu, Y. Penru, A. Guillon, M. Esperanza, C. Miège, J.-M. Choubert, Ozonation of 47 organic micropollutants in secondary treated

municipal effluents: Direct and indirect kinetic reaction rates and modelling, Chemosphere 262 (2021) 127969, https://doi.org/10.1016/j.chemosphere.2020.127969.

[56] S. Willach, H.V. Lutze, K. Eckey, K. Löppenberg, M. Lüling, J. Terhalle, J.-B. Wolbert, M.A. Jochmann, U. Karst, T.C. Schmidt, Degradation of sulfamethoxazole using ozone and chlorine dioxide - compound-specific stable isotope analysis, transformation product analysis and mechanistic aspects, Water Res. 122 (2017) 280–289, https://doi.org/10.1016/j.watres.2017.06.001.

[57] M. Martín-Sómer, C. Pablos, R. van Grieken, J. Marugán, Influence of light distribution on the performance of photocatalytic reactors: Led vs mercury lamps, Appl. Catal. B: Environ. 215 (2017) 1–7, https://doi.org/10.1016/j.apcatb.2017.05.048.

[58] D. Wang, M.A. Mueses, J.A.C. Márquez, F. Machuca-Martínez, I. Grčić, R. PeraltaMunizMoreira, G. LiPuma, Engineering and modeling perspectives on photocatalytic reactors for water treatment, Water Res. 202 (2021) 117421, https://doi.org/10.1016/j.watres.2021.117421.

[59] T.A. Ternes, J. Stüber, N. Herrmann, D. McDowell, A. Ried, M. Kampmann, B. Teiser, Ozonation: a tool for removal of pharmaceuticals, contrast media and musk fragrances from wastewater? Water Res. 37 (8) (2003) 1976–1982, https://doi.org/10.1016/S0043-1354(02)00570-5.

[60] M.M. Huber, A. Göbel, A. Joss, N. Hermann, D. Löffler, C.S. McArdell, A. Ried, H. Siegrist, T.A. Ternes, U. von Gunten, Oxidation of pharmaceuticals during ozonation of municipal wastewater effluents: a pilot study, Environ. Sci. Technol. 39 (11) (2005) 4290–4299, https://doi.org/10.1021/es048396s.

[61] M.N. Sugihara, D. Moeller, T. Paul, T.J. Strathmann, Tio2-photocatalyzed transformation of the recalcitrant x-ray contrast agent diatrizoate, Appl. Catal. B: Environ. 129 (2013) 114–122, https://doi.org/10.1016/j.apcatb.2012.09.013.

[62] J. Radjenovic, V. Flexer, B.C. Donose, D.L. Sedlak, J. Keller, Removal of the x-ray contrast media diatrizoate by electrochemical reduction and oxidation, Environ. Sci. Technol. 47 (23) (2013) 13686–13694, https://doi.org/10.1021/es403410p.

[63] L. Landwehrkamp, A. Kouchaki-Shalmani, C. Forner, R. Hobby, J. Eduful, C. Wagner, Development of efficient characterization parameters for activated carbon used in drinking water treatment, J. Water Supply.: Res. Technol. -Aqua 64 (6) (2015) 688–696, https://doi.org/10.2166/aqua.2015.157.

[64] J. Gomes, J. Lincho, E. Domingues, M. Gmurek, P. Mazierski, A. Zaleska-Medynska, T. Klimczuk, R.M. Quinta-Ferreira, R.C. Martins, Tio2 nanotube arrays-based reactor for photocatalytic oxidation of parabens mixtures in ultrapure water: Effects of photocatalyst properties, operational parameters and light source, Sci. Total Environ. 689 (2019) 79–89, https://doi.org/10.1016/j.scitotenv.2019.06.410.